



PUBLISHED FOR SISSA BY SPRINGER

RECEIVED: October 9, 2012

REVISED: February 12, 2013

ACCEPTED: February 21, 2013

PUBLISHED: March 20, 2013

Next-to-leading-order QCD corrections to the yields and polarisations of J/ψ and Υ directly produced in association with a Z boson at the LHC

Bin Gong,^{a,b} Jean-Philippe Lansberg,^c Cédric Lorcé^{c,d} and Jian-Xiong Wang^{a,b}

^a*Institute of High Energy Physics, CAS,
P.O. Box 918(4), Beijing, 100049, China*

^b*Theoretical Physics Center for Science Facilities, CAS,
19B Yuquanlu, Beijing, 100049, China*

^c*IPNO, Université Paris-Sud, CNRS/IN2P3,
15 rue G. Clemenceau, 91406, Orsay, France*

^d*LPT, Université Paris-Sud, CNRS,
Bâtiment 210, 91405, Orsay, France*

E-mail: twain@ihep.ac.cn, lansberg@in2p3.fr, lorce@ipno.in2p3.fr,
jxwang@ihep.ac.cn

ABSTRACT: We update the study of the production of direct J/ψ in association with a Z boson at the Next-to-Leading Order (NLO) in α_s by evaluating both the yield differential in P_T and the J/ψ polarisation in the QCD-based Colour-Singlet Model (CSM). Contrary to an earlier claim, QCD corrections at small and mid P_T are small if one assumes that the factorisation and the renormalisation scales are commensurate with the Z boson mass. As it can be anticipated, the t -channel gluon-exchange (t -CGE) topologies start to be dominant only for $P_T \gtrsim m_Z/2$. The polarisation pattern is not altered by the QCD corrections. This is thus far the first quarkonium-production process where this is observed in the CSM. Along the same lines, our predictions for direct $\Upsilon + Z$ are also given.

KEYWORDS: QCD Phenomenology, NLO Computations

Contents

1	Introduction	1
2	Cross section at LO accuracy	3
3	Cross section at NLO accuracy	4
3.1	Virtual corrections	4
3.2	Real corrections	5
3.3	NLO [*] cross section	5
4	Results for $J/\psi + Z$: differential cross section in P_T	6
4.1	Comparison with Mao et al. [37]	6
4.2	Results for the differential cross section in P_T at $\sqrt{s} = 8$ TeV and 14 TeV	8
4.3	Scale sensitivity at different P_T	10
5	Polarisation: polar anisotropy in the helicity frame	10
6	Results for $\Upsilon + Z$	12
6.1	Tevatron	12
6.2	LHC	12
7	Conclusions	13

1 Introduction

A few years ago, non-perturbative effects associated with colour-octet (CO) channels [1–3] were considered to be the only plausible explanation for the numerous puzzles in the predictions of quarkonium-production rates at hadron colliders. The situation has slightly changed since then, with the first evaluations of the QCD corrections [4–8] to the yields of J/ψ and Υ (commonly denoted Q hereafter) produced in high-energy hadron collisions via Colour-Singlet (CS) transitions [9–11]. It is now indeed widely accepted [12–14] that α_s^4 and α_s^5 corrections to the CSM are significantly larger than α_s^3 contributions at mid and large P_T and that they should be taken into account in any analysis of their P_T spectrum. Nowadays, it is not clear anymore that CO channels dominate and they are the only source of quarkonia. As a result, there is no consensus on which mechanisms are effectively at work in quarkonium hadroproduction at high energies, that is at RHIC, at the Tevatron and, recently, at the LHC.

Polarisation predictions for the CS channel are also strongly affected by QCD corrections as demonstrated in [6, 8, 15, 16]. At NLO, Q produced inclusively or in association with a photon are expected to be longitudinally polarised when P_T gets larger, whereas

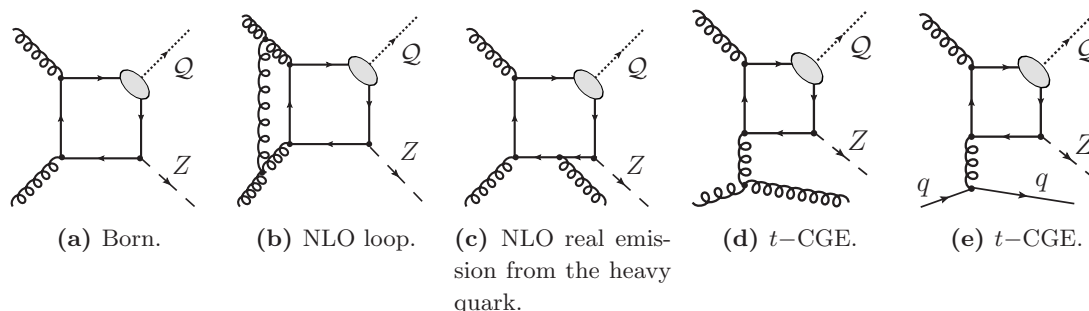


Figure 1. Representative diagrams contributing to J/ψ and Υ (denoted \mathcal{Q}) hadroproduction with a Z boson in the CSM by gluon fusion at orders $\alpha\alpha_s^2$ (a), $\alpha\alpha_s^3$ (b,c,d) and initiated by a light-quark gluon fusion at order $\alpha\alpha_s^3$ (e). The quark and anti-quark attached to the ellipsis are taken as on-shell and their relative velocity v is set to zero.

they were thought to be transversely polarised as predicted at LO in the CSM [17, 18]. Such a drastic change is understood by the dominance of new production topologies. This also explains the significant enhancement in the production rates as observed for increasing P_T .

The situation is rather different at low P_T , where the CS predictions for \mathcal{Q} at LO [9–11] and NLO [4–6] accuracy are of the same magnitude at RHIC energies; this shows a good convergence of the perturbative series. They are also in agreement [19–21] with the existing data from RHIC [22] energy all the way up to that of the LHC [23–30]. CO channels are most likely not needed to account for low P_T data — and thus for the P_T integrated yields. This is at odds with earlier works, e.g. [31], which wrongly assumed that χ_c feed-down could be the dominant CSM contribution. This is supported further by the results of recent works [32–35] focusing on production at e^+e^- colliders which have posed stringent constraints on the size of $C = +1$ CO contributions which can be involved in hadroproduction at low P_T . Finally, this is reminiscent of the broad fixed-target measurement survey of total cross sections [36] which challenged the universality of the CO MEs.

In this paper, we focus on the production of J/ψ (and Υ) in association with a Z boson. Whereas this process may give us complementary information on quarkonium production if it happens to be experimentally accessible at the LHC, it also offers an interesting theoretical playground for the understanding of the QCD corrections in quarkonium-production processes. Our motivation was twofold: first, to see if the polarisation pattern of the J/ψ is altered by the QCD corrections at large P_T ; second, to see how large the effect of new topologies opening at NLO is, by comparing a full NLO computation to a simplified one — NLO * — with a infrared (IR) cut-off and neglecting loops. Our attention has also been drawn to this process by a previous analysis of the yield at NLO [37] which showed an intriguing result where NLO corrections were large at low P_T and getting smaller at large(r) P_T . Such a result could only be explained by a negligible contribution from new kinematically enhanced topologies and a large (positive) contribution from loop corrections at low P_T . As we shall demonstrate, the conclusion drawn in [37] are misguided by an unconventional choice of the factorisation and renormalisation scales (μ_F and μ_R), — way below m_Z — and by a P_T range not large enough — compared to m_Z — to be able to

observe the dominance of t -CGE topologies. As a matter of fact, if one chooses a value for the scales commensurate with m_Z , rather than the transverse mass of the J/ψ as done in [37], the NLO corrections are found to be small at small P_T . On the other hand, for $P_T \gtrsim m_Z/2$, the NLO corrections are enhanced by a kinematical factor P_T^2 .

The paper is organised as follows. In sections 2 and 3, we describe the evaluation of the cross section at LO and NLO accuracy in the CSM. We also explain how the partial NLO^{*} yield is evaluated. In section 4, we present our results which we first compare to those from [37] with the same scale choice, at the same energy and in the same kinematical region. Then, we show our predictions in an extended P_T range for $\mu_{F,R}$ commensurate with m_Z and we discuss the ratio NLO over LO. We also study the sensitivity of our prediction on the aforementioned scales. Afterwards, we compare the NLO^{*} yield with the full NLO and we comment on the dependence on the IR cut-off at large P_T and on the impact of the t -CGE topologies. In section 5, we analyse the yield polarisation at LO, NLO and NLO^{*}. In section 6, we give and discuss our predictions for Υ . Section 7 gathers our conclusions.

2 Cross section at LO accuracy

In the CSM [9–11], the matrix element to create a 3S_1 quarkonium Q with a momentum P_Q and a polarisation λ accompanied by other partons, noted j , and a Z boson of momentum P_Z is the product of the amplitude to create the corresponding heavy-quark pair, $\mathcal{M}(ab \rightarrow Q\bar{Q})$, a spin projector $N(\lambda|s_1, s_2)$ and $R(0)$, the radial wave function at the origin in the configuration space, obtained from the leptonic width, namely

$$\begin{aligned} \mathcal{M}(ab \rightarrow Q^\lambda(P_Q) + Z(p_Z) + j) &= \sum_{s_1, s_2, i, i'} \frac{N(\lambda|s_1, s_2)}{\sqrt{m_Q}} \frac{\delta^{ii'}}{\sqrt{N_c}} \frac{R(0)}{\sqrt{4\pi}} \\ &\times \mathcal{M}(ab \rightarrow Q_i^{s_1} \bar{Q}_{i'}^{s_2}(\mathbf{p} = \mathbf{0}) + Z(p_Z) + j), \end{aligned} \quad (2.1)$$

where $P_Q = p_Q + p_{\bar{Q}}$, $p = (p_Q - p_{\bar{Q}})/2$, s_1 and s_2 are the heavy-quark spins, and $\delta^{ii'}/\sqrt{N_c}$ is the projector onto a CS state. $N(\lambda|s_1, s_2)$ can be written as $\frac{\varepsilon_\mu^\lambda}{2\sqrt{2}m_Q} \bar{v}(\frac{\mathbf{P}_Q}{2}, s_2) \gamma^\mu u(\frac{\mathbf{P}_Q}{2}, s_1)$ in the non-relativistic limit with ε_μ^λ being the polarisation vector of the quarkonium. Summing over the quark spin yields to traces which can be evaluated in a standard way.

At LO, there is only a single partonic process at work, namely $gg \rightarrow J/\psi Z$ — completely analogous to $gg \rightarrow J/\psi \gamma$ for J/ψ -prompt photon associated production — with 4 Feynman graphs to be evaluated. One of them is drawn on figure 1 (a). The differential partonic cross section is readily obtained from the amplitude squared,¹

$$\frac{d\hat{\sigma}}{d\hat{t}} = \frac{1}{16\pi\hat{s}^2} |\mathcal{M}|^2, \quad (2.2)$$

from which one obtains the double differential cross section in P_T ($P_T \equiv P_{J/\psi, T}$) and the J/ψ rapidity, y , for $pp \rightarrow J/\psi Z$ after convolution with the gluon PDFs and a change of

¹The momenta of the initial gluons, $k_{1,2}$, are, as usual in the parton model, related to those of the colliding hadrons ($p_{1,2}$) through $k_{1,2} = x_{1,2} p_{1,2}$. One then defines the Mandelstam variables for the partonic system: $\hat{s} = sx_1x_2$, $\hat{t} = (k_1 - P_{J/\psi})^2$ and $\hat{u} = (k_2 - P_{J/\psi})^2$.

variable:

$$\frac{d\sigma}{dydP_T} = \int_{x_1^{\min}}^1 dx_1 \frac{2\hat{s}P_T g(x_1, \mu_F) g(x_2(x_1), \mu_F)}{\sqrt{s}(\sqrt{s}x_1 - m_T e^y)} \frac{d\hat{\sigma}}{d\hat{t}}, \quad (2.3)$$

where $x_1^{\min} = \frac{m_T \sqrt{s} e^y - m_{J/\psi}^2 + m_Z^2}{\sqrt{s}(\sqrt{s} - m_T e^{-y})}$, $m_T = \sqrt{m_{J/\psi}^2 + P_T^2}$.

3 Cross section at NLO accuracy

The NLO contributions can be divided in two sets: one gathers the virtual corrections which arise from loop diagrams, the other gathers the real (emission) corrections where one more particle appears in the final state. In the next sections, we briefly describe how these are computed.

3.1 Virtual corrections

The computation of the virtual corrections involves three types of singularities: the ultraviolet (UV), the infrared (IR) and the Coulomb ones. UV divergences arising from self-energy and triangle diagrams are cancelled after renormalisation. A similar renormalisation scheme as in ref. [39] is used, except for the fact that, in the present study, the bottom quark is also included in the renormalisation of the gluon field. The renormalisation constants Z_m , Z_2 and Z_3 which are associated to the charm quark mass m_c , the charm field ψ_c and the gluon field A_μ^a are defined in the on-mass-shell (OS) scheme while Z_g , for the QCD gauge coupling constant α_s , is defined in the modified minimal-subtraction ($\overline{\text{MS}}$) scheme taking the dimension $d = 4 - 2\epsilon$:

$$\begin{aligned} \delta Z_m^{OS} &= -3C_F \frac{\alpha_s}{4\pi} \left[\frac{1}{\epsilon_{UV}} - \gamma_E + \ln \frac{4\pi\mu^2}{m_c^2} + \frac{4}{3} \right], \\ \delta Z_2^{OS} &= -C_F \frac{\alpha_s}{4\pi} \left[\frac{1}{\epsilon_{UV}} + \frac{2}{\epsilon_{IR}} - 3\gamma_E + 3 \ln \frac{4\pi\mu^2}{m_c^2} + 4 \right], \\ \delta Z_3^{OS} &= \frac{\alpha_s}{4\pi} \left[(\beta'_0 - 2C_A) \left(\frac{1}{\epsilon_{UV}} - \frac{1}{\epsilon_{IR}} \right) \right. \\ &\quad \left. - \frac{4}{3} T_F \left(\frac{1}{\epsilon_{UV}} - \gamma_E + \ln \frac{4\pi\mu^2}{m_c^2} \right) - \frac{4}{3} T_F \left(\frac{1}{\epsilon_{UV}} - \gamma_E + \ln \frac{4\pi\mu^2}{m_b^2} \right) \right], \\ \delta Z_g^{\overline{\text{MS}}} &= -\frac{\beta_0}{2} \frac{\alpha_s}{4\pi} \left[\frac{1}{\epsilon_{UV}} - \gamma_E + \ln \left(\frac{4\pi\mu^2}{\mu_R^2} \right) \right], \end{aligned} \quad (3.1)$$

where γ_E is Euler's constant, $\beta_0 = \frac{11}{3}C_A - \frac{4}{3}T_F n_f$ is the one-loop coefficient of the QCD beta function and n_f is the number of active quark flavours. We take the three light quarks u, d, s as massless and consider the quarks c and b as heavy; therefore $n_f=5$. In $\text{SU}(3)_c$, we have the following colour factor: $T_F = \frac{1}{2}$, $C_F = \frac{4}{3}$, $C_A = 3$. Finally, $\beta'_0 \equiv \beta_0 + \frac{8}{3}T_F = \frac{11}{3}C_A - \frac{4}{3}T_F n_{lf}$ where $n_{lf} \equiv n_f - 2 = 3$ is the number of light quark flavours.

After having fixed our renormalisation scheme, there are 111 virtual-correction diagrams, including counter-term diagrams. Diagrams that have a virtual gluon line connecting the charm quark pair forming the J/ψ lead to Coulomb singularity $\sim \pi^2/|p|$, which can be isolated and mapped into the $c\bar{c}$ wave function. As dimensional regularisation is

adopted and p is set to zero before loop integrals, the Coulomb singularity automatically disappears in the calculation of the short-distance coefficient.

The loop integration has been carried out thanks to the newly upgraded Feynman Diagram Calculation (FDC) package [40], with the implementation of the reduction method for loop integrals proposed in ref. [41].

3.2 Real corrections

The real corrections arise from three parton-level sub-processes:

$$g + g \rightarrow J/\psi + Z + g, \quad (3.2)$$

$$g + q(\bar{q}) \rightarrow J/\psi + Z + q(\bar{q}), \quad (3.3)$$

$$q + \bar{q} \rightarrow J/\psi + Z + g, \quad (3.4)$$

where q denotes light quarks with different flavours (u, d, s). The charm-gluon fusion contribution may be non-negligible in the presence of intrinsic charm. It will be considered in a separate work.

The contribution from the quark-anti-quark fusion (eq. (3.4)) is IR finite and small. The phase-space integration of the other two sub-processes will generate IR singularities, which are either soft or collinear and which can be conveniently isolated by slicing the phase space into different regions. We use the two-cutoff phase-space-slicing method [42], which introduces two small cutoffs to decompose the phase space into three parts. The real cross section can then be written as

$$\sigma^{\text{Real}} = \sigma^{\text{Soft}} + \sigma^{\text{Hard Collinear}} + \sigma^{\text{Hard Noncollinear}}. \quad (3.5)$$

The hard noncollinear part $\sigma^{\text{Hard Noncollinear}}$ is IR finite and can be numerically computed using standard Monte-Carlo integration techniques. Only the real sub-process of eq. (3.2) contains soft singularities. Collinear singularities appear in both real sub-processes of eq. (3.2) and eq. (3.3), but only as initial-state collinear singularities. As shown in ref. [42], all these singularities can be factored out analytically in the corresponding regions. When combined with the IR singularities appearing in the virtual corrections (see section 3.1), the soft singularities of the real part cancel. Yet, some collinear singularities remain. These are fully absorbed into the redefinition of the parton distribution function (PDF): this is usually referred to as the mass factorisation [43]. All the singularities are thus eventually analytically cancelled. After the cancellation, the dependence on the scale μ vanishes, and the dependences on μ_R and μ_F survives

3.3 NLO* cross section

In order to evaluate the NLO* contributions, we use the framework described in [44] based on the tree-level matrix-element generator MADONIA² slightly tuned to implement an IR cut-off on all light parton-pair invariant mass. The LO cross section has also been checked with MADONIA.

²MADONIA can be used online (model “Quarkonium production in SM”) at [45].

The procedure used here to evaluate the leading- P_T NLO contributions is exactly the same as in [8] but for the process $pp \rightarrow J/\psi + Z + \text{jet}$. Namely, the real-emission contributions at $\alpha\alpha_s^3$ are evaluated using MADONIA by imposing a lower bound on the invariant mass of any light parton pair (s_{ij}^{\min}). The underlying idea in the inclusive³ case was that for the new channels opening up at NLO which have a leading- P_T behaviour w.r.t. to LO ones (for instance the t -CGE), the cut-off dependence should decrease for increasing P_T since no collinear or soft divergences can appear there. For other NLO channels, whose Born contribution is at LO, the cut would produce logarithms of s_{ij}/s_{ij}^{\min} , which are not necessarily negligible. Nevertheless, they can be factorised over their corresponding Born contribution, which scales as P_T^{-8} , and hence are suppressed by at least two powers of P_T with respect to the leading- P_T contributions (P_T^{-6}) at this order. The sensitivity on s_{ij}^{\min} should vanish at large P_T . This argument has been checked in the inclusive case for Υ [8] and ψ [12] as well as in association with a photon [16]. Because of the presence of the Z boson mass, it is not a priori obvious that t -CGE topologies dominate over the LO ones. It is thus not clear at all how such procedure to evaluate the NLO^{*} yield can provide a reliable evaluation of the full NLO of $J/\psi + Z$. In fact, at mid P_T , significantly below the Z boson mass, the difference of the P_T dependence of the NLO and LO cross sections is maybe not large enough for the dependence on s_{ij}^{\min} to decrease fast. Having at hand a full NLO computation, we can carry out such a comparison and better investigate the effect of QCD corrections in quarkonium production. This is done after our complete results are presented.

4 Results for $J/\psi + Z$: differential cross section in P_T

4.1 Comparison with Mao et al. [37]

In order to compare our results with those of [37], we take $\sqrt{s} = 14 \text{ TeV}$ and $|y^{J/\psi}| < 3.0$. We have set the factorisation and renormalisation scales at the same value, namely $\mu_F = \mu_R = m_T^{J/\psi} = \sqrt{m_{J/\psi}^2 + P_T^2}$. For the PDF sets, we used CTEQ6l1 for LO evaluations and CTEQ6m for NLO and NLO^{*} evaluations [46]. We also take $\alpha = 1/137$, $|R_{J/\psi}(0)|^2 = 0.91 \text{ GeV}^3$, $m_c = 1.5 \text{ GeV}$, $m_Z = 91.1876 \text{ GeV}$, and $\sin^2(\theta_W) = 0.23116$. Note that the most up-to-date estimate of the wave function at the origin is actually $|R_{J/\psi}(0)|^2 = 0.944 \text{ GeV}^3$ as extracted from the leptonic decay widths of J/ψ [38]. Our LO results (also cross-checked with MADONIA) do match with those of [37] (compare both blue curves on figure 2). However, as depicted in figure 2, we are not able to reproduce the NLO results presented in [37].⁴ At low P_T , we have found a K factor smaller than one (i.e. the yield at NLO is smaller than at LO) while they obtained a value larger than one.

That being said, a scale close to m_Z , rather than the transverse mass of the J/ψ taken in [37], seems more appropriate as done for instance for $Z + b$ -jet [47]. This has an important effect on the scale sensitivity, less on the final numbers predicted for the yields, as we shall discuss in the next section.

³“Inclusive” is used here in opposition to “in association with another detected particle” which is indeed a more exclusive process.

⁴See, however, the note added on page 14.

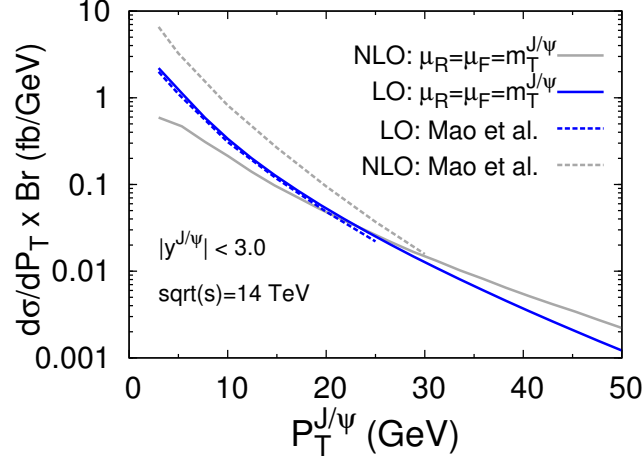


Figure 2. Comparison between our results (solid lines) and that of Mao et al. [37] (dashed lines) for the differential cross section for $J/\psi + Z$ vs. the J/ψ P_T at LO (blue) and NLO (grey) with $\mu_F = \mu_R = m_T^{J/\psi}$.

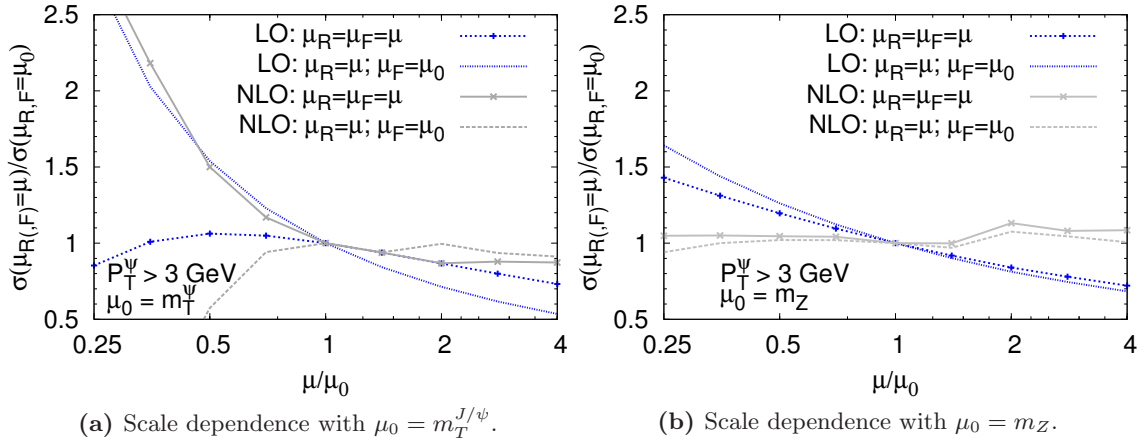


Figure 3. (a) Renormalisation and factorisation scale dependence of the LO and NLO yield for $P_T > 3$ GeV with $\mu_0 = m_T^{J/\psi}$. (b) Same plot as (a) for $\mu_0 = m_Z$.

In figure 3, we show the scale sensitivity at low P_T around two different choices of the “default” scale value, μ_0 , (a) the transverse mass of the J/ψ and (b) the Z boson mass. We emphasise that we believe the latter choice to be more appropriate owing to the presence of the Z boson in the hard process. One sees that around m_Z (b), the cross section at NLO is more stable, except for a bump at m_t which can be corrected by properly setting the value of $\Lambda^{[6]}$ in the running of coupling constant (currently 0.151 MeV with $m_t = 180$ GeV), which matters for $\mu_R > m_t$. The NLO results are clearly unstable at low scales and they may then artificially be enhanced. In the following sections, we investigate further the dependence of the scale sensitivity for different domains of the J/ψ transverse momenta.

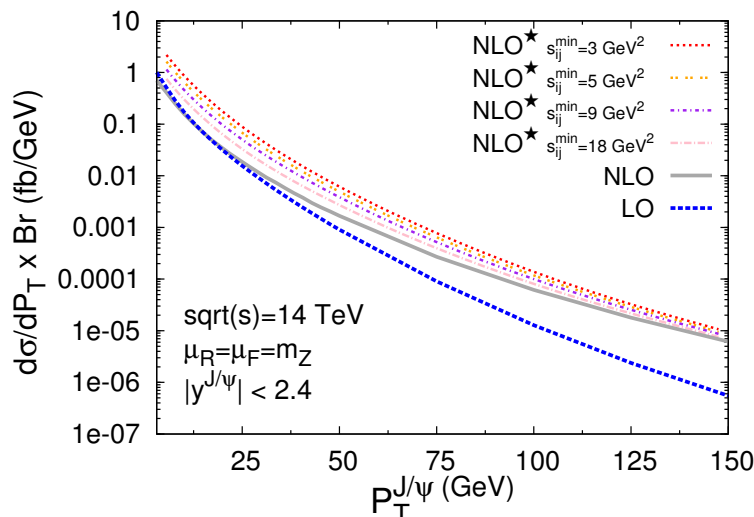


Figure 4. Differential cross section for $J/\psi + Z$ vs. P_T at $\sqrt{s} = 14$ TeV at LO (blue dashed) and NLO (grey solid) with $\mu_F = \mu_R = m_Z$ along with the NLO* for different values of s_{ij}^{\min} (red dotted, yellow double dotted, purple dash dotted and pink long-dash dotted).

4.2 Results for the differential cross section in P_T at $\sqrt{s} = 8$ TeV and 14 TeV

In the following, we show our results for $|y^{J/\psi}| < 2.4$ — the usual J/ψ acceptance for the CMS and ATLAS detectors — at 8 TeV and⁵ 14 TeV and for the renormalisation and factorisation scales set at m_Z . We have kept⁶ the cut $P_T^{J/\psi} > 3$ GeV.

The parameters entering the evaluation of the cross section have been taken as follows: $|R_{J/\psi}(0)|^2 = 0.91 \text{ GeV}^3$, $\text{Br}(J/\psi \rightarrow \ell^+\ell^-) = 0.0594$, $m_c = 1.5 \text{ GeV}$ with $m_{J/\psi} = 2m_c$, $m_b = 4.75 \text{ GeV}$, $\alpha = 1/128$. Our result at $\sqrt{s} = 14$ TeV are depicted on figure 4. The dotted blue line is our LO result and the solid grey line is our prediction at NLO. It is obvious, contrary to what was obtained in [37], that the yield at NLO is getting larger than at LO for increasing P_T . This is similar to what happens in the inclusive case. This is also indicative that new leading P_T topologies, in particular t -CGE, start dominating rather early in P_T despite of the presence of a Z boson in the process. At $P_T = 150 \text{ GeV}$, the NLO yield is already ten times that of LO.

The dominance of t -CGE topologies can be quantified by a comparison with the results from the NLO* evaluation. As aforementioned, because of the Z boson mass, it was not a priori clear that the NLO* evaluation could make any sense here. Indeed, as long as the contribution from the sub-leading P_T topologies are significant, the NLO* would strongly depend on the arbitrary IR cutoff⁷ which is used to mimic the effect of the loop contributions which regulate the soft-gluon-emission divergences. We are in a position to

⁵The cross section at 13 TeV is 12 % smaller than at 14 TeV.

⁶Note that we could have evaluated the cross section for lower P_T where the cross section is well behaved. However, we do not expect — at least in the central region — any experimental measurement to be carried out in this region owing to the momentum cut on the muons because of the strong magnetic fields in the ATLAS and CMS detectors.

⁷Not to be confused with the cutoff used in the full NLO computation, on which the final results does not depend.

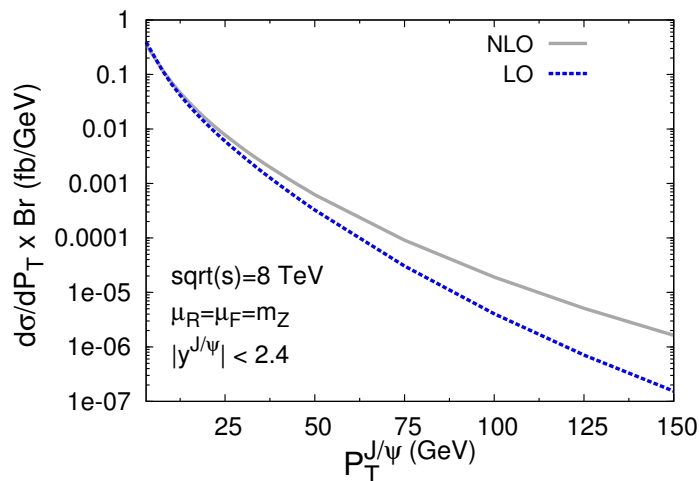


Figure 5. Differential cross section for $J/\psi + Z$ vs. P_T at $\sqrt{s} = 8$ TeV at LO (blue dashed) and NLO (grey solid) with $\mu_F = \mu_R = m_Z$.

check from which P_T the NLO* starts to reproduce the full NLO and becomes to be less sensitive on the IR cut.

The various dotted lines on figure 4 show the NLO* evaluation for different cut-off values. Two observations can be made: 1) they converge to the NLO steadily for increasing P_T , 2) for $P_T > m_Z$, the NLO* evaluations are within a factor of 2 compatible with the complete NLO yield. This confirms that loop corrections are sub-leading in P_T and can be safely neglected for P_T larger than all the masses relevant for the process under consideration and that new topologies appearing at NLO, the t -CGE ones, dominate at large P_T . At low P_T , where the NLO and LO yield are similar, the NLO* overestimate the NLO.

As regards the possibility to study such a process at the LHC, the P_T differential cross sections times the branching $\text{Br}(J/\psi \rightarrow \mu^+ \mu^-)$ at the smallest P_T accessible by ATLAS and CMS (3 to 5 GeV depending on the rapidity) is of the order of 1 fb/GeV at 14 TeV (figure 4) and three times less at 8 TeV (figure 5). These do not take into account the branching of the Z in dimuons ($\sim 3\%$). In the most optimistic case, by integrating on the accessible P_T range, by using both muon and electron decay channels for the J/ψ , by expecting an indirect cross section of 40 % and by detecting the Z boson with hadronic channels such that it could be detected 40 % of the time, it may be envisioned to detect something like four hundred events at 14 TeV with 100 fb^{-1} of data. At 8 TeV with the 20 fb^{-1} of data expected to be collected in 2012, we expect only about thirty events to be recorded. Clearly, there are more promising processes, such as $J/\psi + \gamma$ [15, 16] or $J/\psi + D$ [19, 48], to learn more on the production mechanisms of the J/ψ . Nevertheless, the study of $J/\psi + Z$ may suffer less from trigger limitations and could thus still be at reach at the LHC. In any case, it is an ideal theory playground to analyse the effects of QCD corrections on quarkonium production, which have been the key subject in the recent years in the field.

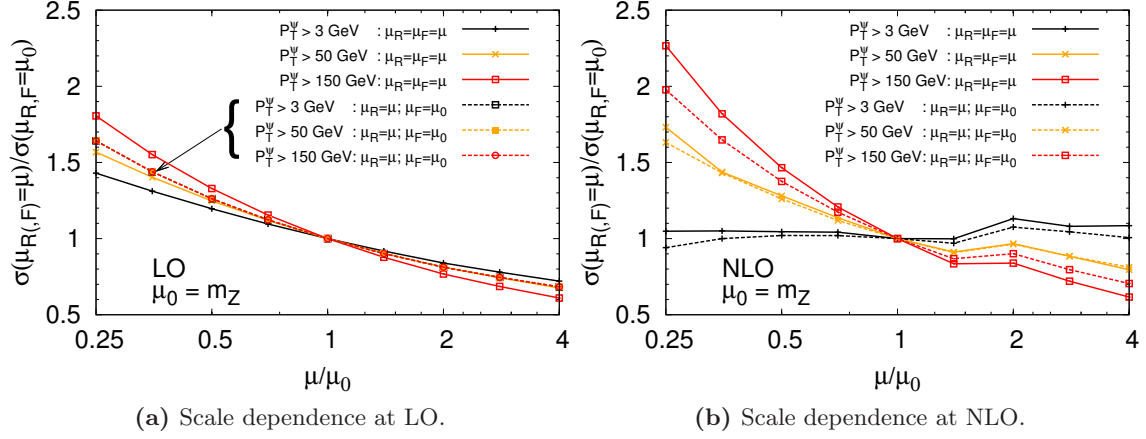


Figure 6. Scale dependence of the yield at LO (a) and NLO (b) for $P_T > 3$ GeV, $P_T > 50$ GeV, $P_T > 150$ GeV where both the renormalisation and factorisation scales are varied together ($\mu_F = \mu_R$, solid lines) about $\mu_0 = m_Z$ and only the renormalisation scale is varied (μ_F fixed, dashed lines). Note that α has been kept fixed.

4.3 Scale sensitivity at different P_T

From the observations made above, we expect the real emission contributions at $\alpha\alpha_s^3$ to dominate for $P_T \gtrsim m_Z/2$. This should therefore impact on the scale dependence of the yield. At low P_T ($\ll m_Z$), we expect a reduced scale dependence since we really deal with a process at NLO accuracy. At large P_T , the leading process is $pp \rightarrow J/\psi + Z + \text{parton}$. The loop contributions are not expected to reduce the scale sensitivity since they are small. On the contrary, we expect a larger sensitivity on the renormalisation scale, μ_R , since the leading process shows an additional power of $\alpha_s(\mu_R)$. In practice, we study the scale sensitivity by varying μ_F and μ_R together and then μ_R alone by a factor 2 about the “default” scale m_Z with 3 cuts in P_T — i.e. 3, 50 and 150 GeV.

On figure 6, we do observe, as anticipated for $P_T \gtrsim m_Z$ (red curves), a stronger scale sensitivity of the NLO yield (b) — at $\alpha\alpha_s^3$ — than of the LO yields (a) — at $\alpha\alpha_s^2$. The NLO curve with μ_F fixed clearly shows that the sensitivity essentially comes from μ_R . At mid P_T (orange curves), the scale sensitivities are similar at LO and NLO, while at low P_T (black curves), the NLO yield is less scale dependent than the LO — in agreement with the common wisdom regarding the NLO computations. Note also that the 3 LO curves showing the sole dependence on μ_R are identical since one can factor out a common α_s^2 since our choices of μ_R do not depend on P_T .

5 Polarisation: polar anisotropy in the helicity frame

The polar anisotropy of the dilepton decay of the J/ψ , λ_θ or α , can be evaluated from the polarised hadronic cross sections:

$$\alpha(P_T) = \frac{\frac{d\sigma_T}{dP_T} - 2\frac{d\sigma_L}{dP_T}}{\frac{d\sigma_T}{dP_T} + 2\frac{d\sigma_L}{dP_T}}. \quad (5.1)$$

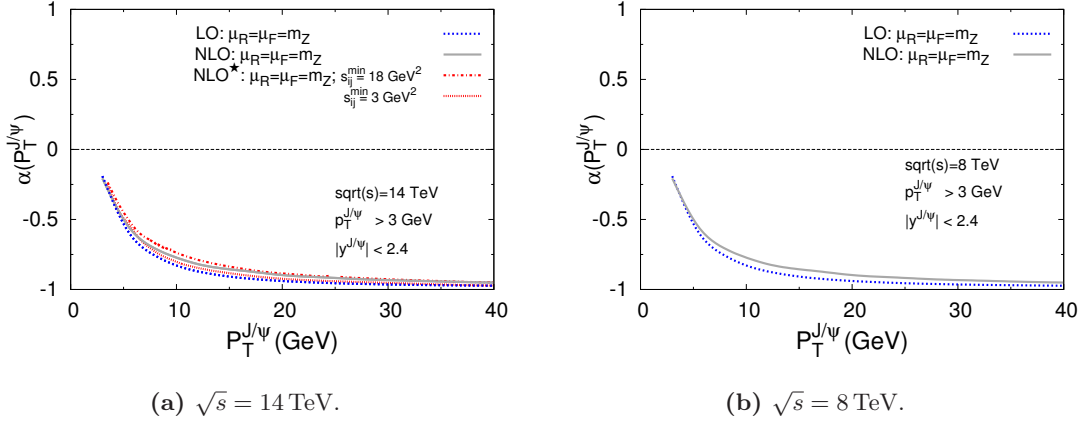


Figure 7. (a) P_T dependence of the polarisation (or azimuthal anisotropy) in the helicity frame of the direct J/ψ produced with a Z boson at LO, NLO and NLO* (for 2 values of the IR cut-off) at $\sqrt{s} = 14$ TeV. (b) Same as (a) at LO and NLO at $\sqrt{s} = 8$ TeV.

To evaluate $\alpha(P_T)$, the polarisation of J/ψ must of course be kept throughout the calculation. The partonic differential cross section for a polarised J/ψ is expressed as:

$$\frac{d\hat{\sigma}_\lambda}{d\hat{t}} = a \, \epsilon(\lambda) \cdot \epsilon^*(\lambda) + \sum_{i,j=1,2} a_{ij} \, p_i \cdot \epsilon(\lambda) \, p_j \cdot \epsilon^*(\lambda), \quad (5.2)$$

where $\lambda = T_1, T_2, L$. $\epsilon(T_1)$, $\epsilon(T_2)$, $\epsilon(L)$ are respectively the two transverse and the longitudinal polarisation vectors of J/ψ ; the polarisations of all the other particles are summed over. One can find that a and a_{ij} are finite when the virtual and real corrections are properly handled as aforementioned. There is therefore no difference in the partonic differential cross section $d\hat{\sigma}_\lambda/d\hat{t}$ whether the polarisation of J/ψ is summed over in 4 or n dimensions. Thus, we can just treat the polarisation vectors of J/ψ in 4 dimensions. There are usually several different choices of the polarisation frames, as discussed in refs. [49–51]. In our calculation, we have chosen to work in the helicity frame. The polarisation can be obtained in a given frame by taking the corresponding polarisation vectors in eq. (5.2).

Our results at 14 TeV in figure 7 (a) clearly show that the direct- J/ψ yield in association with a Z boson is increasingly longitudinally polarised in the helicity frame for increasing $P_T^{J/\psi}$. The NLO and NLO* results coincide and the latter is nearly insensitive to the IR cutoff. Interestingly, the NLO and the LO results are also very similar. This is the first time that such a robustness of the polarisation against QCD corrections is observed for the colour-singlet channels. For the J/ψ produced inclusively or in association with a photon, the yield at LO and NLO are found to have a completely different polarisation. Our interpretation is that, when a Z boson is emitted by one of the charm quarks forming the J/ψ , the latter is longitudinally polarised, irrespective of the off-shellness and of the transverse momentum of the gluons producing the charm-quark pair. This is not so when a photon or a gluon is emitted in the final state. In the present case, we also note that the polarisation at 8 TeV (figure 7 (b)) is nearly exactly the same as at 14 TeV.

6 Results for $\Upsilon + Z$

Along the same lines as for J/ψ , we have also evaluated the cross section and the polarisation for direct- Υ production in association with a Z boson. We have set the factorisation and renormalisation scales at the same value, namely $\mu_F = \mu_R = m_Z$, and we used the same PDF sets as for the $J/\psi + Z$ case. We also have taken $\alpha = 1/128$, $|R_\Upsilon(0)|^2 = 7.6 \text{ GeV}^3$, $m_b = 4.75 \text{ GeV}$, $m_Z = 91.1876 \text{ GeV}$, and $\sin^2(\theta_W) = 0.23116$.

6.1 Tevatron

Experimentally, the CDF Collaboration at Fermilab has set a 95 % C.L. upper value for such a cross section at $\sqrt{s} = 1.8 \text{ TeV}$ [52], namely

$$\sigma(p\bar{p} \rightarrow \Upsilon + Z + X) \times \text{Br}(\Upsilon \rightarrow \mu^+ \mu^-) < 2.5 \text{ pb}. \quad (6.1)$$

Further studies with the entire data set recorded by CDF is under process [53]. At $\sqrt{s} = 1.8 \text{ TeV}$, a quick evaluation of the total cross section (without y cut, nor P_T cut) gives, for the CSM, a value close to 0.1 fb ($\sim 0.2 \text{ fb}$ by taking into account a similar feed-down fraction ($\sim 50\%$) to that of the inclusive case). A similar evaluation for the CO transitions is highly dependent on the chosen LDME values and on the expected impact of the feed-down. Values span from $\sim 0.06 \text{ fb}$ for the direct yield with CO LDMEs fit [54] from the early prompt Tevatron data, up to $\sim 3.75 \text{ fb}$ as evaluated in [55], passing by $\sim 0.4 \text{ fb}$ for the direct yield using CO LDMEs fit from the latest Tevatron results taking into account some NLO QCD corrections [56]. This is, in any case, significantly below the CDF upper bound obtained with 83 pb^{-1} of data. Given these small theoretical values, we fear that such process cannot be experimentally accessed at the Tevatron, unless contributions from colour-octet transitions, from double-parton interactions or from feed-downs are unexpectedly large.

6.2 LHC

At the LHC at 14 TeV , the expected yield in the CSM for the central rapidity region accessible by CMS and ATLAS is of the order 5 fb (still including the branching of the Υ in muons). The central values for the differential cross sections vs. P_T at LO and NLO are shown in figures 8 (a-c). An enhancement by a factor 2 to 4 can certainly be expected if the feed-downs from excited bottomonium states and the usual theoretical uncertainties are taken into account.

By comparing figures 8 (a-c), one also notices an interesting phenomenon: the NLO and LO yields start to depart from each other at low P_T for increasing \sqrt{s} . This can probably be attributed to an increasing — negative — size of the loop corrections in this region at small x . This is in fact reminiscent to what has been observed in the inclusive case [4, 6, 19, 20]. In the latter case, the situation is worse since the NLO cross section can become negative for large \sqrt{s} and small P_T .

For the sake of the comparison with the J/ψ case, we have also computed the polarisation at LO and NLO. As it can be seen on figure 9, the yield polarisation at LO and

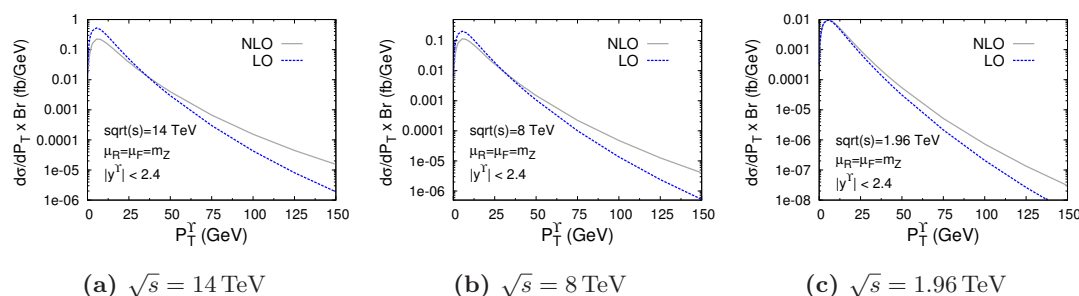


Figure 8. Differential cross section for direct $\Upsilon + Z$ vs. P_T at LO (blue-dashed) and NLO (grey-solid) with $\mu_F = \mu_R = m_Z$ at 14 TeV (a), 8 TeV (b) and⁸ 1.96 TeV (c).

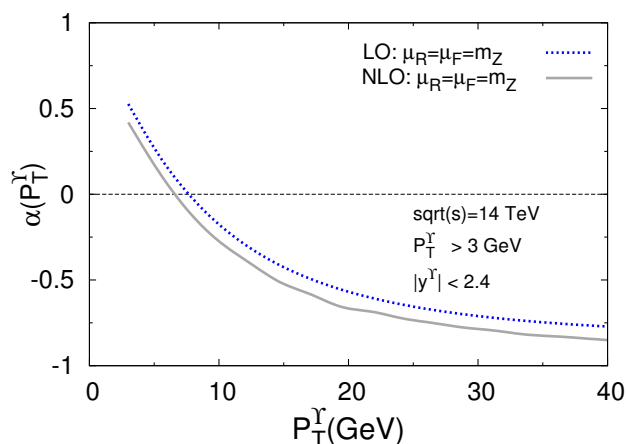


Figure 9. P_T dependence of the polarisation (or azimuthal anisotropy) in the helicity frame of the direct Υ produced with a Z boson at LO and NLO at $\sqrt{s} = 14$ TeV.

NLO are very alike, though slightly different from for the J/ψ case — most probably due to the change in the quarkonium mass compared to the Z mass.

7 Conclusions

In conclusion, we have studied the effects of the QCD corrections to the production of direct J/ψ and Υ via colour-singlet transitions in association with a Z boson at the LHC. We have found, contrary to an earlier study [37], that the NLO QCD corrections are consistent with the expectations, namely increasing for increasing P_T and small at low P_T . We expect that a few hundred $J/\psi + Z$ events could be detected at the LHC at 14 TeV with 100 fb^{-1} of data. At 8 TeV with 20 fb^{-1} , there may be just enough events to derive a cross section and not only an upper bound on its value. Interestingly, the CSM yield expected for direct $\Upsilon + Z$ is of the same order of magnitude than that of direct $J/\psi + Z$ at 14 TeV, if not larger.

⁸We have considered a wider rapidity range than usual for the CDF quarkonium analyses since CMX muons can be used in such a correlation analysis owing to the smaller background compared to inclusive measurements [53].

We have studied the scale sensitivity of the $J/\psi + Z$ cross section at LO and NLO. At low P_T , it is smaller when QCD corrections are taken into account. On the contrary, at large P_T , i.e. when $P_T \gtrsim m_Z/2$, the dominant contributions are of the kind of $gg \rightarrow Q + Z + \text{jet}$. These involve an additional power of α_s and the sensitivity on the renormalisation scale is larger. That being said, the presence of the Z boson mass renders the CSM prediction more precise at low P_T compared to the inclusive case, for which the leading- P_T contributions at NLO dominate at lower P_T .

We have also found that the yield polarisation is not altered by the QCD corrections. From this observation, we have concluded that when a Z boson is emitted by one of the heavy quarks forming the quarkonium, both the J/ψ and the Υ are longitudinally polarised at LO and NLO, thus independently of the off-shellness and of the transverse momentum of the gluons producing the heavy-quark pair. This is at odds with the cases of inclusive Q production and $Q + \gamma$ production, and this motivates further theoretical and experimental investigations.

Note added. During the publication process, Mao et al. submitted an erratum where some of their results are corrected [57]. Their NLO results now agree with ours. However, we still disagree with their choice of μ_R and μ_F .

Acknowledgments

This work is supported in part by the France-China Particle Physics Laboratory, by the P2I network and by the National Natural Science Foundation of China (Nos. 10979056 and 11005137).

Open Access. This article is distributed under the terms of the Creative Commons Attribution License which permits any use, distribution and reproduction in any medium, provided the original author(s) and source are credited.

References

- [1] M. Kramer, *Quarkonium production at high-energy colliders*, *Prog. Part. Nucl. Phys.* **47** (2001) 141 [[hep-ph/0106120](#)] [[INSPIRE](#)].
- [2] QUARKONIUM WORKING GROUP collaboration, N. Brambilla et al., *Heavy quarkonium physics*, CERN Yellow Report 2005-005, CERN, Geneva Switzerland (2005) [[hep-ph/0412158](#)] [[INSPIRE](#)].
- [3] J. Lansberg, *J/ψ , ψ' and Υ production at hadron colliders: a review*, *Int. J. Mod. Phys. A* **21** (2006) 3857 [[hep-ph/0602091](#)] [[INSPIRE](#)].
- [4] J.M. Campbell, F. Maltoni and F. Tramontano, *QCD corrections to J/ψ and Υ production at hadron colliders*, *Phys. Rev. Lett.* **98** (2007) 252002 [[hep-ph/0703113](#)] [[INSPIRE](#)].
- [5] P. Artoisenet, J. Lansberg and F. Maltoni, *Hadroproduction of J/ψ and Υ in association with a heavy-quark pair*, *Phys. Lett. B* **653** (2007) 60 [[hep-ph/0703129](#)] [[INSPIRE](#)].

- [6] B. Gong and J.-X. Wang, *Next-to-leading-order QCD corrections to J/ψ polarization at Tevatron and Large-Hadron-Collider energies*, *Phys. Rev. Lett.* **100** (2008) 232001 [[arXiv:0802.3727](#)] [[INSPIRE](#)].
- [7] B. Gong and J.-X. Wang, *QCD corrections to polarization of J/ψ and Υ at Tevatron and LHC*, *Phys. Rev. D* **78** (2008) 074011 [[arXiv:0805.2469](#)] [[INSPIRE](#)].
- [8] P. Artoisenet, J.M. Campbell, J. Lansberg, F. Maltoni and F. Tramontano, *Υ production at Fermilab Tevatron and LHC energies*, *Phys. Rev. Lett.* **101** (2008) 152001 [[arXiv:0806.3282](#)] [[INSPIRE](#)].
- [9] C.-H. Chang, *Hadronic production of J/ψ associated with a gluon*, *Nucl. Phys. B* **172** (1980) 425 [[INSPIRE](#)].
- [10] R. Baier and R. Ruckl, *Hadronic production of J/ψ and Υ : transverse momentum distributions*, *Phys. Lett. B* **102** (1981) 364 [[INSPIRE](#)].
- [11] R. Baier and R. Ruckl, *Hadronic collisions: a quarkonium factory*, *Z. Phys. C* **19** (1983) 251 [[INSPIRE](#)].
- [12] J. Lansberg, *On the mechanisms of heavy-quarkonium hadroproduction*, *Eur. Phys. J. C* **61** (2009) 693 [[arXiv:0811.4005](#)] [[INSPIRE](#)].
- [13] N. Brambilla et al., *Heavy quarkonium: progress, puzzles and opportunities*, *Eur. Phys. J. C* **71** (2011) 1534 [[arXiv:1010.5827](#)] [[INSPIRE](#)].
- [14] Z. Conesa del Valle et al., *Quarkonium production in high energy proton-proton and proton-nucleus collisions*, *Nucl. Phys. Proc. Suppl.* **214** (2011) 3 [[arXiv:1105.4545](#)] [[INSPIRE](#)].
- [15] R. Li and J.-X. Wang, *Next-to-leading-order QCD corrections to $J/\psi(\Upsilon) + \gamma$ production at the LHC*, *Phys. Lett. B* **672** (2009) 51 [[arXiv:0811.0963](#)] [[INSPIRE](#)].
- [16] J. Lansberg, *Real next-to-next-to-leading-order QCD corrections to J/ψ and Υ hadroproduction in association with a photon*, *Phys. Lett. B* **679** (2009) 340 [[arXiv:0901.4777](#)] [[INSPIRE](#)].
- [17] A.K. Leibovich, *ψ' polarization due to color octet quarkonia production*, *Phys. Rev. D* **56** (1997) 4412 [[hep-ph/9610381](#)] [[INSPIRE](#)].
- [18] C. Kim and E. Mirkes, *Testing J/ψ production and decay properties in hadronic collisions*, *Phys. Rev. D* **51** (1995) 3340 [[hep-ph/9407318](#)] [[INSPIRE](#)].
- [19] S.J. Brodsky and J.-P. Lansberg, *Heavy-quarkonium production in high energy proton-proton collisions at RHIC*, *Phys. Rev. D* **81** (2010) 051502 [[arXiv:0908.0754](#)] [[INSPIRE](#)].
- [20] J. Lansberg, *Total J/ψ and Υ production cross section at the LHC: theory vs. experiment*, *PoS(ICHEP2010)206* [[arXiv:1012.2815](#)] [[INSPIRE](#)].
- [21] J. Lansberg, *Υ production in pp and pA collisions: from RHIC to the LHC*, [[arXiv:1209.0331](#)] [[INSPIRE](#)].
- [22] PHENIX collaboration, A. Adare et al., *J/ψ production versus transverse momentum and rapidity in $\bar{p}p$ collisions at $\sqrt{s} = 200$ GeV*, *Phys. Rev. Lett.* **98** (2007) 232002 [[hep-ex/0611020](#)] [[INSPIRE](#)].
- [23] STAR collaboration, B. Abelev et al., *Υ cross section in $p + p$ collisions at $\sqrt{s} = 200$ GeV*, *Phys. Rev. D* **82** (2010) 012004 [[arXiv:1001.2745](#)] [[INSPIRE](#)].

- [24] CDF collaboration, D. Acosta et al., Υ production and polarization in $p\bar{p}$ collisions at $\sqrt{s} = 1.8$ TeV, *Phys. Rev. Lett.* **88** (2002) 161802 [[INSPIRE](#)].
- [25] D0 collaboration, V. Abazov et al., Measurement of inclusive differential cross sections for Υ_{1S} production in $p\bar{p}$ collisions at $\sqrt{s} = 1.96$ TeV, *Phys. Rev. Lett.* **94** (2005) 232001 [Erratum *ibid.* **100** (2008) 049902] [[hep-ex/0502030](#)] [[INSPIRE](#)].
- [26] CMS collaboration, Measurement of the inclusive Υ production cross section in pp collisions at $\sqrt{s} = 7$ TeV, *Phys. Rev. D* **83** (2011) 112004 [[arXiv:1012.5545](#)] [[INSPIRE](#)].
- [27] ATLAS collaboration, Measurement of the Υ_{1S} production cross-section in pp collisions at $\sqrt{s} = 7$ TeV in ATLAS, *Phys. Lett. B* **705** (2011) 9 [[arXiv:1106.5325](#)] [[INSPIRE](#)].
- [28] LHCb collaboration, Measurement of Υ production in pp collisions at $\sqrt{s} = 7$ TeV, *Eur. Phys. J. C* **72** (2012) 2025 [[arXiv:1202.6579](#)] [[INSPIRE](#)].
- [29] LHCb collaboration, Measurement of J/ψ production in pp collisions at $\sqrt{s} = 7$ TeV, *Eur. Phys. J. C* **71** (2011) 1645 [[arXiv:1103.0423](#)] [[INSPIRE](#)].
- [30] ALICE collaboration, Rapidity and transverse momentum dependence of inclusive J/ψ production in pp collisions at $\sqrt{s} = 7$ TeV, *Phys. Lett. B* **704** (2011) 442 [Erratum *ibid.* **B 718** (2012) 692] [[arXiv:1105.0380](#)] [[INSPIRE](#)].
- [31] F. Cooper, M.X. Liu and G.C. Nayak, J/ψ production in pp collisions at $\sqrt{s} = 200$ GeV at RHIC, *Phys. Rev. Lett.* **93** (2004) 171801 [[hep-ph/0402219](#)] [[INSPIRE](#)].
- [32] Z.-G. He, Y. Fan and K.-T. Chao, Relativistic correction to $e^+e^- \rightarrow J/\psi + gg$ at B factories and constraint on color-octet matrix elements, *Phys. Rev. D* **81** (2010) 054036 [[arXiv:0910.3636](#)] [[INSPIRE](#)].
- [33] Y.-J. Zhang, Y.-Q. Ma, K. Wang and K.-T. Chao, QCD radiative correction to color-octet J/ψ inclusive production at B factories, *Phys. Rev. D* **81** (2010) 034015 [[arXiv:0911.2166](#)] [[INSPIRE](#)].
- [34] Y.-Q. Ma, Y.-J. Zhang and K.-T. Chao, QCD correction to $e^+e^- \rightarrow J/\psi gg$ at B factories, *Phys. Rev. Lett.* **102** (2009) 162002 [[arXiv:0812.5106](#)] [[INSPIRE](#)].
- [35] B. Gong and J.-X. Wang, Next-to-leading-order QCD corrections to $e^+e^- \rightarrow J/\psi + gg$ at the B factories, *Phys. Rev. Lett.* **102** (2009) 162003 [[arXiv:0901.0117](#)] [[INSPIRE](#)].
- [36] F. Maltoni et al., Analysis of charmonium production at fixed-target experiments in the NRQCD approach, *Phys. Lett. B* **638** (2006) 202 [[hep-ph/0601203](#)] [[INSPIRE](#)].
- [37] S. Mao, M. Wen-Gan, L. Gang, Z. Ren-You and G. Lei, QCD corrections to J/ψ plus Z^0 -boson production at the LHC, *JHEP* **02** (2011) 071 [Erratum *ibid.* **12** (2012) 010] [[arXiv:1102.0398](#)] [[INSPIRE](#)].
- [38] B. Gong and J.-X. Wang, QCD corrections to double J/ψ production in e^+e^- annihilation at $\sqrt{s} = 10.6$ GeV, *Phys. Rev. Lett.* **100** (2008) 181803 [[arXiv:0801.0648](#)] [[INSPIRE](#)].
- [39] B. Gong and J.-X. Wang, Next-to-leading-order QCD corrections to $e^+e^- \rightarrow J/\psi c\bar{c}$ at the B factories, *Phys. Rev. D* **80** (2009) 054015 [[arXiv:0904.1103](#)] [[INSPIRE](#)].
- [40] J.-X. Wang, Progress in FDC project, *Nucl. Instrum. Meth. A* **534** (2004) 241 [[hep-ph/0407058](#)] [[INSPIRE](#)].
- [41] G. Duplancic and B. Nizic, Reduction method for dimensionally regulated one loop N point Feynman integrals, *Eur. Phys. J. C* **35** (2004) 105 [[hep-ph/0303184](#)] [[INSPIRE](#)].

- [42] B. Harris and J. Owens, *The two cutoff phase space slicing method*, *Phys. Rev. D* **65** (2002) 094032 [[hep-ph/0102128](#)] [[INSPIRE](#)].
- [43] G. Altarelli, R.K. Ellis and G. Martinelli, *Large perturbative corrections to the Drell-Yan process in QCD*, *Nucl. Phys. B* **157** (1979) 461 [[INSPIRE](#)].
- [44] P. Artoisenet, F. Maltoni and T. Stelzer, *Automatic generation of quarkonium amplitudes in NRQCD*, *JHEP* **02** (2008) 102 [[arXiv:0712.2770](#)] [[INSPIRE](#)].
- [45] *Generate processes online using MadGraph 5 webpage*, <http://madgraph.hep.uiuc.edu/>.
- [46] J. Pumplin et al., *New generation of parton distributions with uncertainties from global QCD analysis*, *JHEP* **07** (2002) 012 [[hep-ph/0201195](#)] [[INSPIRE](#)].
- [47] J.M. Campbell, R.K. Ellis, F. Maltoni and S. Willenbrock, *Associated production of a Z boson and a single heavy quark jet*, *Phys. Rev. D* **69** (2004) 074021 [[hep-ph/0312024](#)] [[INSPIRE](#)].
- [48] LHCb collaboration, *Observation of double charm production involving open charm in pp collisions at $\sqrt{s} = 7$ TeV*, *JHEP* **06** (2012) 141 [[arXiv:1205.0975](#)] [[INSPIRE](#)].
- [49] M. Beneke, M. Krämer and M. Vanttinen, *Inelastic photoproduction of polarized J/ψ* , *Phys. Rev. D* **57** (1998) 4258 [[hep-ph/9709376](#)] [[INSPIRE](#)].
- [50] P. Faccioli, C. Lourenco, J. Seixas and H.K. Wohri, *Towards the experimental clarification of quarkonium polarization*, *Eur. Phys. J. C* **69** (2010) 657 [[arXiv:1006.2738](#)] [[INSPIRE](#)].
- [51] P. Faccioli, *Questions and prospects in quarkonium polarization measurements from proton-proton to nucleus-nucleus collisions*, *Mod. Phys. Lett. A* **27** (2012) 1230022 [[arXiv:1207.2050](#)] [[INSPIRE](#)].
- [52] CDF collaboration, D. Acosta et al., *Search for associated production of Υ and vector boson in $p\bar{p}$ collisions at $\sqrt{s} = 1.8$ TeV*, *Phys. Rev. Lett.* **90** (2003) 221803 [[INSPIRE](#)].
- [53] M. Kruse, A. Limosani and C. Zhou, private communications.
- [54] P.L. Cho and A.K. Leibovich, *Color octet quarkonia production. 2*, *Phys. Rev. D* **53** (1996) 6203 [[hep-ph/9511315](#)] [[INSPIRE](#)].
- [55] E. Braaten, J. Lee and S. Fleming, *Associated production of Υ and weak gauge bosons at the Tevatron*, *Phys. Rev. D* **60** (1999) 091501 [[hep-ph/9812505](#)] [[INSPIRE](#)].
- [56] B. Gong, J.-X. Wang and H.-F. Zhang, *QCD corrections to Υ production via color-octet states at the Tevatron and LHC*, *Phys. Rev. D* **83** (2011) 114021 [[arXiv:1009.3839](#)] [[INSPIRE](#)].
- [57] S. Mao, M. Wen-Gan, L. Gang, Z. Ren-You and G. Lei, *QCD corrections to J/ψ plus Z^0 -boson production at the LHC*, *JHEP* **02** (2011) 071 [Erratum *ibid.* **12** (2012) 010] [[arXiv:1102.0398](#)] [[INSPIRE](#)].